Chemical Characterization, Source Apportionment, and Health Risk Assessment of PM2.5 in a Typical Industrial Region in North China

zhanshan wang (18701650609@163.com)
Beijing
Jiayi Yan
Chinese Academy of Forestry
Puzhen Zhang
Chinese Academy of Sciences
Zhigang Li
Chinese Academy of Sciences
Chen Guo
Chinese Academy of Sciences
Kai Wu
Chinese Academy of Sciences
Xiaoqian Li
Chinese Academy of Sciences
Xiaojing Zhu
Chinese Academy of Sciences
Zhaobin Sun
Chinese Academy of Sciences
Yongjie Wei
Chinese Academy of Sciences

Research Article

Keywords: North China, PM2.5, chemical composition, source apportionment, SOC, health risk assessment

Posted Date: December 8th, 2021

DOI: https://doi.org/10.21203/rs.3.rs-1088131/v1

Abstract

To clarify the chemical characteristics, source contributions, and health risks of pollution events associated with high $PM_{2.5}$ in typical industrial areas of North China, manual sampling and analysis of $PM_{2.5}$ were conducted in the spring, summer, autumn, and winter of 2019 in Pingyin County, Jinan City, Shandong Province. The results showed that the total concentration of 29 components in $PM_{2.5}$ was 53.4 $\mu g \cdot m^{-3}$; the largest contribution was from the NO_3^- ion, at 14.6 ± 14.2 $\mu g \cdot m^{-3}$, followed by organic carbon (OC), SO_4^{2-}, and NH_4^+, with concentrations of 9.3 ± 5.5, 9.1 ± 6.4, and 8.1 ± 6.8 $\mu g \cdot m^{-3}$, respectively. The concentrations of OC, NO_3^-, and SO_4^{2-} were highest in winter and lowest in summer, whereas the NH_4^+ concentration was highest in winter and lowest in spring. Typical heavy metals had higher concentrations in autumn and winter, and lower concentrations in spring and summer. The annual average sulfur oxidation rate (SOR) and nitrogen oxidation rate (NOR) were 0.30 ± 0.14 and 0.21 ± 0.12, respectively, with the highest SO_2 emission and conversion rates in winter, resulting in the SO_4^{2-} concentration being highest in winter. Although the emission rate of SO_2 was low in summer, its conversion rate was high. In winter and autumn, NORs were significantly higher than in spring and summer, and a higher NOR in autumn contributed to significant elevation of the NO_3^- concentration in autumn relative to spring and summer. The average concentration of secondary organic carbon in 2019 was 2.8±1.9 $\mu g \cdot m^{-3}$, and it comprised approximately 30% of total OC. The health risk assessment for typical heavy metals showed that Pb poses a potential carcinogenic risk for adults, whereas As may pose a carcinogenic risk for adults, children, and adolescents. Positive matrix factorization analysis indicated that coal-burning emissions contributed the largest fraction of $PM_{2.5}$, accounting for 35.9% of the total. The contribution of automotive emissions is similar to that of coal, at 32.1%. The third-largest contributor was industrial sources, which accounted for 17.2%. The contributions of dust and other emissions sources to $PM_{2.5}$ were 8.4% and 6.4%, respectively.

1. Introduction

The North China Plain (NCP) is one of the most heavily atmospherically polluted areas in China. From a geographical perspective, the North China Plain is located between the Yanshan Mountains in the north, Taihang Mountains in the west, and Bohai Bay in the east, which create a semi-closed topography with high-elevation terrain in the northwest and low-elevation terrain in the southeast. Due to this configuration, air pollutants are easily transmitted into the area, but do not readily diffuse out. From a meteorological perspective, periods of drought with little rainfall in northern China weaken wet deposition onto the NCP. Although the northwest monsoon is strong in winter, the mountains to the northwest of the NCP weaken the removal effect of pollutants by the monsoon, and the overall wind speed is low, inhibiting the diffusion of air pollutants. Heavy emissions from industrial processes, coal-burning emissions from energy production, and traffic emissions in North China contribute to the high emission levels of atmospheric pollutants (Jia et al., 2021; Luo et al., 2021; Wu et al., 2020; Zhang et al., 2020a). Particulate matter is one of the major pollutants in the NCP.

Particulate matter, especially $PM_{2.5}$ (particulate matter consisting of fine particles with aerodynamic diameters of less than 2.5 μm), plays important roles in the atmosphere, such as driving visibility reduction, acid deposition, and climate change (Cheng et al., 2021; Liu et al., 2019; Liu et al., 2021a; Nguyen et al., 2019; Zhang et al., 2020c; Zhao et al., 2020a). $PM_{2.5}$ is also associated with adverse health effects. Exposure to high concentrations of $PM_{2.5}$ has been found to result in increases in hospitalization and mortality rates (Honda et al., 2020; Lurie et al., 2019; Sugiyama et al., 2020; Zhang et al., 2020b). Research to characterize $PM_{2.5}$ in the NCP has been conducted over the last two decades. Several studies have examined the general characteristics of chemical components in $PM_{2.5}$ and discussed their seasonal variations (Lim et al., 2020; Liu et al., 2021b; Wei et al., 2020; Yi et al., 2021; Zhao et al., 2020b). Investigations have focused on correlations between $PM_{2.5}$ components and the formation of secondary particles (Dong et al., 2020; Du et al., 2019; Wang et al., 2020; Yang et al., 2020). The evolutionary processes and formation mechanisms of heavy $PM_{2.5}$ pollution have been discussed (Guo et al., 2020a; Hu et al., 2021; Li et al., 2020a; Shi et al., 2020). Several studies have aimed to reveal the regional transportation and source apportionment of $PM_{2.5}$ (Feng et al., 2016; Wang et al., 2016; Yao et al., 2016; Zong et al., 2018). In addition, lidar, satellite remote sensing, and numerical simulation have been used to investigate $PM_{2.5}$ pollution (He et al., 2020; Li et al., 2020b; Lin et al., 2018; Lv et al., 2017).

Most previous studies have focused on the urban or background area of the NCP. The present study was conducted in Pingyin County, Jinan City, Shandong Province, which is located in the middle of the NCP and is a typical industrial area. Chemical characterization, source analysis, and a health risk assessment of $PM_{2.5}$ were conducted to provide reference data for policymakers to improve the air quality in the NCP.

2. Materials And Methods

2.1 Sample collection

Manual sampling was conducted in the spring (20 May–11 June), summer (17 July–2 August), autumn (30 October–14 November), and winter (December) of 2019 at an air-quality monitoring station in Huaihai Yushu, Pingyin County, with samples collected over 15 days in spring, summer and autumn, and 30 days in winter. The sampling periods included a total of 84 days, accounting for approximately one-quarter of the total days in the year. The ambient air particulate matter sampler instrument was produced by Dandong Baite Company and has been certified by the China National Environmental Monitoring Centre. One Teflon membrane and one quartz membrane (47-mm Whatman filters) were collected from two sets of instruments per sampling event. The sampling period was 23 h, with 1 h for membrane replacement, and a blank membrane was taken every 15 days. A total of 168 membrane samples were obtained. The ratio of organic carbon (OC) to elemental carbon (EC), nine water-soluble ions, and 18 elements were analyzed for each membrane filter. The sampling location is shown in Fig. 1.

2.2 Analytical methods

1. Ion analysis

In this study, the water-soluble ions F^-, Cl^-, NO_3^-, SO_4^{2-}, Na^+, K^+, Mg^{2+}, Ca^{2+}, and NH_4^+ were analyzed with reference to the national standards HJ 799-2016 (2016) and HJ 800 (2016). A quarter of a quartz membrane filter was smashed, immersed in 10 ml of deionized water, shaken uniformly, and extracted for 15 min in an ultrasonic bath. The supernatant was removed after 5 min of settling and analyzed using Dionex ICS-2100 and ICS-1100 ion chromatographs.

2. OC/EC analysis

OC and EC were measured using a USA Sunset Lab RT-4 carbon analyzer. The samples were not pre-treated. After the quartz membrane was removed from the refrigerator and allowed to come to room temperature, the analyzer was used to directly measure OC and EC.

3. Element analysis

In this study, 18 elements were analyzed, including Na, Mg, and Al. First, a Teflon membrane was placed into a clean sample digestion tank for digestion, then 20 ml of saturated boric acid solution was added for the complexation of excessive F^- ions, and closed microwave digestion was carried out. After digestion, the volume was adjusted to 50 ml. Element analysis was conducted using an Intrepid-XDL spectrometer.

In addition, SO_2 and NOx concentrations were monitored synchronously using 100E and 200E SO_2 analyzers produced by the API Corporation of America.

2.3 Health risk assessment

Heavy metal elements can enter the human body and endanger human health through three pathways: the skin, digestive system, and respiratory system. The heavy metal elements in $PM_{2.5}$ mainly enter the human body through the respiratory system. In this study, four heavy metals registered with the United States Agency for Toxic Substances and Disease Registry¾As, Mn, Ni, and Pb¾were selected from the monitored metals for analysis. The potential exposure risk was analyzed using the pollutant exposure model recommended by the United States Environmental Protection Agency (US EPA). The formula for calculating the exposure dose is as follows:

$$ADD(LADD) = C \times IR \times EF \times ED / (BW \times AT),$$

where ADD is the non-carcinogenic exposure dose with units of mg/(kg·d), LADD is the lifetime average exposure dose of carcinogens (mg/[kg·d]), C is the concentration of heavy metals (mg/m^3), IR is the respiratory rate (m^3/d), EF is the exposure frequency (d/a), ED is the exposure duration (a), BW is body mass (kg), and AT is the average exposure time (d). The values of these parameters are shown in Table 1 (US EPA and Ministry of Ecology and Environment of the People's Republic of China) (Bi et al., 2020; Li et al., 2021).

Table 1 Exposure parameters for heavy metals entering the human body through the respiratory system

Population	Age range (years)	IR (m^3/d)	EF (d/a)	ED (a)	BW (kg)	AT to non-carcinogenic materials (d)	AT to carcinogenic materials (d)
Adult males	18–70	16.6	365	30	67.3	30×365	70×365
Adult females	18–70	13.5	365	30	57.5	30×365	70×365
Children and adolescents	6–17	8.7	365	18	46	18×365	70×365

The carcinogenic risk index and non-carcinogenic risk index through respiratory exposure were calculated as follows:

R_1 = ADD/RfD

R_2 = LADD×SF,

where R_1 is the non-carcinogenic risk of a pollutant associated with respiratory exposure, R_2 is the carcinogenic risk of a pollutant associated with respiratory exposure, RfD is the reference dose (mg/[kg·d]), and SF is the carcinogenic intensity coefficient of a carcinogenic pollutant (kg·d/mg). When $R_1 \leq 1$, the non-carcinogenic health risk is negligible; when $R_1 > 1$, the pollutant poses a non-carcinogenic risk. When $R_2 < 10^{-6}$, the carcinogenic risk is negligible, when R_2 is between 10^{-6} and 10^{-4}, there is a potential carcinogenic risk; when $R_2 > 10^{-4}$, there is a high carcinogenic risk. The values of RfD and SF are shown in Table 2 (US EPA and Ministry of Ecology and Environment of the People's Republic of China) (Chen et al., 2015; Zhai et al., 2014).

Table 2 Dose-response parameters of heavy metals entering the human body through the respiratory pathway

Heavy metal element	RfD (mg/[kg·d])	SF (kg·d/mg)
As	3.0×10^{-4}	15.1
Mn	3.0×10^{-4}	—
Ni	2.0×10^{-2}	1.19
Pb	3.5×10^{-3}	0.28

2.4 Source contribution analysis

The sources of $PM_{2.5}$ were analyzed using the positive matrix factorization (PMF) receptor model. First, the error associated with the chemical component weights of the receptor was determined, and then the main sources of contamination and their contribution ratios were determined using the least squares method. PMF is a type of multivariate factor analysis in which a mathematical method is used to

decompose matrix X containing sample data for a species into two matrices: factor contributions (G) and factor spectra (F). The method does not require the input of a source spectrum and ensures that the decomposition factor contribution (G) and factor spectrum (F) are non-negative (Jain et al., 2020; Lv et al., 2021; Manousakas et al., 2017; Padoan et al., 2020). The matrix X can be represented by the following formula：

$$x_{ij} = \sum_{k=1}^{p} g_{ik} f_{kj} + e_{ij},$$

where Xij is the concentration of species j in sample i, p is the number of factor, gik is the contribution of factor k to sample i, *f*kj is the concentration of factor k in species j, and eij is the error of species j in sample i.

3. Results And Discussion

3.1 $PM_{2.5}$ component concentrations

The concentrations of $PM_{2.5}$ components during the sampling period are shown in Figure 2. The total concentration of 29 components was 53.4 μg·m^{-3}, with the largest contribution from the NO_3^- ion, which had an average concentration of 14.6 ± 14.2 μg·m^{-3}, followed by OC, SO_4^{2-}, and NH_4^+, with average concentrations of 9.3 ± 5.5, 9.1 ± 6.4, and 8.1 ± 6.8 μg·m^{-3}, respectively. These four components were the main contributors to $PM_{2.5}$, and the sum of their concentrations accounted for 76.7% of the total concentration of 29 components. Among other components, the concentrations of EC and water-soluble ions such as Cl^- and K^+ were between 0.2 ± 0.1 and 2.2 ± 1.5 μg·m^{-3}, with Mg^{2+} having the lowest concentration among components, and EC having the highest concentration. The concentrations of 18 elements including Na, Mg, and Al were between 2.3 ± 1.6 and 888.1 ± 415.2 ng·m^{-3}, with Ni having the lowest concentration and K the highest.

The monitoring results of this study were compared with those of other observational studies conducted in Jinan City, and the summary of the comparison is shown in Table 3. The concentrations of SO_4^{2-}, NO_3^-, and NH_4^+ (SNA) in 2019 were significantly lower than the concentrations from monitoring in 2015, especially for SO_4^{2-}. On the other hand, relative to monitoring results from 2016 and 2017 in Jinan, including background and urban areas, no reduction in SNA concentrations was apparent in 2019, when the NO_3^- concentration reached its highest level. Due mainly to the high level of industrial activity in Pingyin County and its associated emissions, the overall $PM_{2.5}$ concentration for the county was higher than the level for Jinan City. Compared with monitoring results from Jinan City in 2011, 2014, and 2016–2017, the concentration of Mn was lowest in 2019, during which the second-lowest concentrations of Ni and Pb were also observed, and As was near its lowest observed concentration. Overall, the concentrations of typical heavy metals in $PM_{2.5}$ in Pingyin County declined significantly from the

previous years, based on monitoring results from those years. Comprehensive analysis of these results indicates that NO_3^- pollution in Pingyin County is serious.

Table 3 Concentrations of chemical components of $PM_{2.5}$ in Jinan from previous studies

Reference	Sampling period	Sampling site classification	Component concentration ($\mu g \cdot m^{-3}$)				
			OC	EC	NO_3^-	SO_4^{2-}	NH_4^+
This study	Spring, summer, autumn, and winter of 2019	Jinan industrial region	9.3	2.2	14.6	9.1	8.1
Zhang et al. (2019)	Throughout the year 2017	Jinan urban area	9.10	2.68	13.55	12.85	7.89
Bie et al. (2019)	Spring, summer, autumn, and winter of 2016	Jinan background area	10.0	1.0	14.3	10.9	9.5
Liu et al. (2018)	Summer and winter of 2015	Jinan urban area	13.5	5.1	15.4	22.9	13.1
Reference	Sampling period	Sampling site classification	Component concentration ($ng \cdot m^{-3}$)				
			Mn	Ni	As	Pb	
This study	Spring, summer, autumn, and winter of 2019	Jinan industrial region	23.7	2.3	7.1	68.2	
Gao et al. (2019)	2016–2017	Jinan City district	27.5	2.0	6.2	62.5	
Yin et al. (2020)	May, October, and December of 2011	Jinan urban area	54.0	4.1	6.7	76.1	
Zhang et al. (2015)	November 2014	Jinan urban area	31	2.0	10.0	79.0	

3.2 Seasonal variations in $PM_{2.5}$ components

Fig. 3 shows the average variations in the concentrations of the main components of $PM_{2.5}$ in Pingyin County among seasons. The concentrations of OC, NO_3^-, and SO_4^{2-} were highest in winter and lowest in summer. The mean concentration of OC was higher in winter (13.8 ± 5.7 $\mu g \cdot m^{-3}$) than in autumn (8.9 ± 2.6 $\mu g \cdot m^{-3}$), spring (7.5 ± 2.0 $\mu g \cdot m^{-3}$), or summer (3.5 ± 2.3 $\mu g \cdot m^{-3}$). OC is mainly derived from the

combustion of fossil fuels, and its concentration is elevated in winter due to emissions from the burning of coal for heating. High concentrations of OC in autumn and spring are generally related to biomass combustion (Ikemori et al., 2021; Khan et al., 2021; Ren et al., 2021). The mean concentration of NO_3^- was higher in winter (23.4 ± 15.0 μg·m^{-3}) than in autumn (19.9 ± 13.5 μg·m^{-3}), spring (5.1 ± 3.1 μg·m^{-3}), or summer (3.1 ± 3.0 μg·m^{-3}). NO_3^- mainly originates from the emissions of motor vehicle exhaust and industrial processes. The concentrations of NO_3^- were significantly higher in autumn and winter than in spring and summer in Pingyin County, indicating that industrial emissions have a strong influence on NO_3^-. The average concentration of SO_4^{2-} was greater in winter (12.4 ± 7.6 μg·m^{-3}) than in autumn (8.2 ± 4.0 μg·m^{-3}), spring (7.1 ± 4.3 μg·m^{-3}), or summer (5.7 ± 4.7 μg·m^{-3}). SO_4^{2-} mainly arises through the conversion of SO_2 from coal-fired emissions. In contrast with OC and NO_3^-, concentrations of SO_4^{2-} were similar in summer, spring, and autumn. Although SO_2 emissions are low in summer, the high temperatures and humidity are favorable for the generation of SO_4^{2-} (Wang et al., 2019a; Yang et al., 2018). NH_4^+ exhibited a different seasonal pattern, with higher concentrations in summer than in spring. The mean concentration of NH_4^+ was higher in winter (12.1 ± 6.7 μg·m^{-3}) than in autumn (9.8 ± 5.7 μg·m^{-3}), summer (3.2 ± 1.8 μg·m^{-3}), or spring (2.2 ± 1.6 μg·m^{-3}). NH_4^+ mainly originates from coal combustion, agricultural production, and organic matter degradation. The high concentration of NH_4^+ in summer may be related to the high temperatures, which increases the volatility of NH_3 and its rate of chemical conversion (Pandolfi et al., 2012). For typical heavy metals, overall concentrations were higher in autumn and winter, and lower in spring and summer. The concentrations of Mn and Pb were similar, with no seasonal variation apparent. The concentration of Ni was similar in spring, summer, and autumn, and higher in winter. The concentration of As was highest in autumn, lowest in summer, and similar in winter and spring.

3.3 Sulfur oxidation rate and nitrogen oxidation rate

The sulfur oxidation rate (SOR) and nitrogen oxidation rate (NOR) are used to indicate the degrees of conversion of SO_2 and NO_2 in the atmosphere, respectively, and are defined as SOR = ρ (SO_4^{2-})/(ρ[SO_4^{2-}] + ρ[SO_2]) and NOR = ρ (NO_3^-)/(ρ[NO_3^-] + ρ[NO_2]). Higher SOR and NOR values indicate greater oxidation of gaseous pollutants and the generation of more SO_4^{2-} and NO_3^- (Ding et al., 2019; Guo et al., 2020b). Fig. 4 shows SORs and NORs in different seasons in Pingyin County. Throughout the year, the mean SOR and NOR were 0.30 ± 0.14 and 0.21 ± 0.12, respectively. The NO_3^- concentration in Pingyin County was higher than the SO_4^{2-} concentration. Whereas, sulfur underwent oxidation at a higher rate than did nitrogen. In autumn, the NOR was greater than the SOR, but it was lower than the SOR in spring, summer, and winter. Seasonal variations in the SOR and NOR were observed. The SOR was higher in winter (0.35 ± 0.14) than in summer (0.31 ± 0.18), spring (0.27 ± 0.11), or autumn (0.25 ± 0.09), and the highest concentration of SO_4^{2-} was observed in winter. Although SO_2 emissions are low in summer, the conversion rate is high. The SOR was similar in spring and autumn. The NOR was higher in winter (0.27 ± 0.11) than in autumn (0.27

± 0.12), spring (0.15 ± 0.06), or summer (0.11 ± 0.09), with similar levels in winter and autumn that were higher than the values in spring and summer. The high NOR in autumn is likely one driver of the high NO_3^- concentration in autumn relative to spring and summer.

3.4 Secondary OC estimation

The OC/EC ratio is often used to characterize the emission and transformation of carbon aerosols and to evaluate and identify secondary sources of particulate matter. EC, which mainly arises from incomplete combustion of carbonaceous fuel, is stable and does not participate in chemical reactions in the atmosphere. Therefore, it is used as a tracer for primary anthropogenic emissions. OC includes primary OC (POC), which is directly discharged from emission sources, as well as secondary OC (SOC), which is generated by photochemical reactions. Chow et al. (1996) argued that an OC/EC ratio > 2 indicates conditions under which SOC can be generated in the atmosphere, whereas Castro et al. (1999) proposed that SOC can be generated when the OC/EC ratio is > 1.1. In addition to photochemical reactions, biomass burning releases a large amount of OC and its effect on EC is relatively small, leading to a high OC/EC ratio. Zhang et al. (2007) found that the average OC/EC in China reached 7.7 when grain straw was burned.

As the complicated atmospheric formation processes and condensation/distribution mechanisms of SOC remain unclear, no unified analytical method is available for the direct measurement of SOC. In addition to directly simulating SOC generation under specific conditions in an aerosol chamber, SOC concentrations in the atmospheric environment are generally estimated through indirect methods, such as calculation from the OC/EC concentration ratio, the organic molecular tracing method, and the numerical model prediction method. Among these methods, the one based on the OC/EC ratio is the simplest and most direct and has been widely applied to identify and assess SOC pollution.

In the OC/EC-ratio method, the OC/EC concentration ratio of particulates emitted from pollution sources is considered to be relatively stable and associated with the emission source. When the OC/EC ratio of atmospheric particles exceeds this characteristic stable value, SOC formation is likely. According to this theory, Turpin and Huntzicker (1995) proposed the following formula for calculating SOC:

$$\mathrm{SOC} = \mathrm{TOC} - \mathrm{EC} \times (\mathrm{OC/EC})_{\mathrm{pri}},$$

where TOC represents total OC, and $(OC/EC)_{pri}$ represents the average OC/EC ratio in the pollution source, which is difficult to determine and associated with high uncertainty. Estimating the ratio requires understanding the emission characteristics of each pollution source in the region and the consideration of daily and seasonal fluctuations in both emissions and meteorological conditions. Due to this difficulty, Castro et al. (1999) proposed the following formula to estimate SOC based on minimum OC/EC values:

$$\mathrm{SOC} = \mathrm{TOC} - \mathrm{EC} \times (\mathrm{OC/EC})_{\mathrm{min}}$$

The OC/EC ratios in different seasons in Pingyin County, the SOC concentrations estimated using this method, and SOC/OC ratios are shown in Fig. 5. These results revealed an annual average OC/EC ratio of 4.7 ± 1.1, indicating the presence of SOC generation. The OC/EC ratio was higher in spring (5.4 ± 0.7) than in autumn (5.3 ± 0.6), winter (4.4 ± 0.8), or summer (3.8 ± 2.0), with the higher values in spring and autumn indicating biomass combustion. The average SOC concentration over Pingyin County was 2.8 ± 1.9 $\mu g \cdot m^{-3}$ throughout the year, and the seasonal SOC concentrations were 4.0 ± 2.0 $\mu g \cdot m^{-3}$ in winter, 3.3 ± 2.0 $\mu g \cdot m^{-3}$ in summer, 1.7 ± 0.7 $\mu g \cdot m^{-3}$ in spring, and 1.6 ± 0.9 $\mu g \cdot m^{-3}$ in autumn. Although the OC concentration was low in summer, the SOC concentration was high then. The annual average SOC/OC ratio was 0.3 ± 0.2, which indicates that approximately 30% of the OC concentration in Pingyin County was SOC generated through secondary chemical reactions, whereas the proportion of POC was approximately 70%. The SOC/OC ratio was 0.6 ± 0.3 in summer, 0.3 ± 0.1 in winter, 0.2 ± 0.1 in spring, and 0.2 ± 0.1 in autumn. Thus, the SOC/OC ratio was highest in summer, and lowest in spring and autumn.

3.5 Health risk assessment of heavy metals

The carcinogenic and non-carcinogenic risk coefficients for four heavy metals were calculated, and the results are shown in Fig. 6. The non-carcinogenic risk coefficients for all heavy metals were lower than 1, indicating that the non-carcinogenic risk was negligible. No risk of cancer was associated with Mn, and the carcinogenic risk coefficient for Ni was less than 10^{-6}, indicating negligible risk. The risk coefficient associated with Pb exposure in children and adolescents was less than 10^{-6}, indicating negligible risk, but the carcinogenic risk coefficient for adults was between 10^{-6} and 10^{-4}, indicating a potential risk due to Pb. The carcinogenic risk coefficient associated with As exposure in adults and children and adolescents was between 10^{-6} and 10^{-4}, indicating that both groups face potential risk. From the comparison among groups, the carcinogenic and non-carcinogenic risk coefficients associated with heavy metals were greatest for adult males, followed by adult females, and were lowest for children and adolescents.

3.6 $PM_{2.5}$ source contribution analysis

$PM_{2.5}$ sources were classified into coal, traffic, dust, industry, and other sources based on the $PM_{2.5}$ source analysis results published by the Jinan municipal government. Fig. 7 shows the spectra of various sources based on the optimal solution of the PMF model. For factor 1, the contributions of secondary components such as SO_4^{2-}, NO_3^-, and NH_4^+ were high; therefore, this factor was considered the secondary source factor. For factor 2, the contributions of Na, S, P, and other elements were high, which is characteristic of chemical production emissions (Wang et al., 2021); therefore, this factor was considered to represent industrial sources. For factor 3, the contribution of the element Zn was the highest, indicating traffic emissions (Hao et al., 2019), and the high contents of OC and EC also support its designation as the traffic source factor. For factor 4, the contributions of crustal elements such as Al, Si, Ca, and Fe were high, so it was identified as the dust source factor. For factor 5, Cl^- made the greatest contribution, which

is characteristic of coal emissions (Sawlani et al., 2021), and the OC concentration was high, indicating that this factor represents coal combustion.

Fig. 8(a) shows the contributions of various $PM_{2.5}$ sources in Pingyin County based on the PMF results. The largest contribution was from secondary sources, which accounted for 45.4%, followed by coal-fired sources at 24.9%, traffic sources at 17.5%, and dust and industrial sources, which accounted for 8.4% and 3.8%, respectively. From the PMF analytical results, secondary sources were attributed to primary sources based on an atmospheric pollution source emission inventory for Pingyin County, and the final results are shown in Fig. 8(b). Coal-fired sources contributed the most to $PM_{2.5}$ in the region, accounting for 35.9% of the total; traffic sources contributed a similar amount as coal-fired sources, at 32.1%. The third-largest contributor was industrial sources, which accounted for 17.2%. The contributions of dust and other emission sources to $PM_{2.5}$ were 8.4% and 6.4%, respectively. Thus, emissions from coal and traffic sources contributed the most to $PM_{2.5}$, and therefore, the regulation of coal burning and traffic emissions should be strengthened to improve air quality in Pingyin County. In this study, coal-fired sources include coal-fired industrial activities, whereas industrial sources refer to non-coal-fired industries.

Limitations

This study had some limitations. The first limitation is the representativeness of the sampling period, as this study did not involve uninterrupted sampling through 2019. The length of the sampling period in spring, summer, and autumn was 15 days, which may not fully reflect the characteristics of each season. Second, there were more sampling days in winter (twice the number in the other seasons), because heavy pollution events occur frequently over the NCP in winter and we decided to sample at a higher frequency. This unevenness in the number of sampling days might have led to the overestimation of the overall pollution level of the region. The respiratory inhalation pathway was analyzed in this study in the heavy metal health risk assessment, but toxic substances in the air can also enter the human body through other pathways. Thus, the overall risk to human health might have been underestimated in this study.

Conclusion

In 2019, the total concentration of 29 components of $PM_{2.5}$ over Pingyin County was 53.4 $\mu g \cdot m^{-3}$, with the largest contribution from NO_3^- (14.6 ± 14.2 $\mu g \cdot m^{-3}$), followed by OC, SO_4^{2-}, and NH_4^+, which had average concentrations of 9.3 ± 5.5, 9.1 ± 6.4, and 8.1 ± 6.8 $\mu g \cdot m^{-3}$, respectively. Compared with observation results from 2016 and 2017 from monitoring the background and urban areas of Jinan City, the concentration of $PM_{2.5}$ over Pingyin County did not decrease significantly in 2019, whereas the concentration of NO_3^- reached its highest level. The concentrations of OC, NO_3^-, and SO_4^{2-} were highest in winter and lowest in summer. The concentration of NH_4^+ was higher in summer than in spring. Typical heavy metal concentrations were higher in autumn and winter than in spring and summer.

The SOR and NOR were 0.30 ± 0.14 and 0.21 ± 0.12, respectively, in 2019. Aside from autumn, when the NOR was greater than the SOR, the SOR was higher than the NOR in all other seasons. The mean NO_3^- concentration over Pingyin County was higher than the SO_4^{2-} concentration, whereas the mean NOR was lower than the mean SOR. The emission and conversion rate of SO_2 were highest in winter, resulting in winter having the highest concentration of SO_4^{2-}. Although SO_2 emission was low in summer, the conversion rate was high. The NOR in winter and autumn was similar, and values in those seasons were significantly higher than in spring and summer; the high NOR in autumn might have caused the high NO_3^- concentration in autumn relative to spring and summer.

The annual average concentration of SOC in 2019 was estimated to be 2.8 ± 1.9 $\mu g \cdot m^{-3}$, and SOC concentrations were 4.0 ± 2.0, 3.3 ± 2.0, 1.7 ± 0.7, and 1.6 ± 0.9 $\mu g \cdot m^{-3}$ in winter, summer, spring, and autumn, respectively. Although the OC concentration was low in summer, the SOC concentration was higher in summer than in other seasons. In 2019, approximately 30% of the OC concentration comprised SOC, which is produced through secondary chemical reactions. The health risk assessment of typical heavy metal elements showed that Pb poses a potential carcinogenic risk for adults, and As poses potential carcinogenic risks for adults, children, and adolescents.

The results of PMF analysis showed that coal-burning sources contributed the largest fraction of total $PM_{2.5}$, at 35.9%, whereas the contribution from traffic sources was similar, at 32.1%. The third-largest contributor to $PM_{2.5}$ was industrial sources, which accounted for 17.2% of the total. The contributions of dust and other emission sources to $PM_{2.5}$ were 8.4% and 6.4%, respectively. Coal-burning and traffic emissions were the largest contributors to $PM_{2.5}$ in this region. Therefore, policymakers should take steps to control coal-burning and traffic emissions to reduce the concentration of $PM_{2.5}$ in typical industrial areas in the NCP, such as adopting measures to increase the proportion of clean energy, eliminate inefficient coal-fired boilers, promote renewable-energy vehicles, and upgrade the emission standards for motor vehicles.

Declarations

Data availability. The data are available on request to the lead corresponding author.

Funding. This work was funded by the National Natural Science Foundation of China (No. 41705112).

Author information

Affiliations

State Key Laboratory of Environmental Criteria and Risk Assessment, Chinese Research Academy of Environmental Sciences, Beijing, 100012, China

Zhanshan Wang, Puzhen Zhang, Zhigang Li, Chen Guo, Xiaoqian Li, Xiaojing Zhu & Yongjie Wei

The ecological environment monitoring center of Linyi, Shandong province, Linyi, 276000, China

Jiayi Yan

Plateau Atmosphere and Environment Key Laboratory of Sichuan Province, School of Atmospheric Sciences, Chengdu University of Information Technology, Chengdu, 610225, China

Department of Land, Air, and Water Resources, University of California, Davis, CA, USA

Kai Wu

Institute of Urban Meteorology, China Meteorological Administration, Beijing, 100089, China

Zhaobin Sun

Contributions

Zhanshan Wang: Conceptualization, Methodology, Formal analysis, Investigation, Writing - original draft, Visualization.

Zhigang Li and Chen Guo: Conceptualization, Validation, Investigation, Writing - review & editing.

Kai Wu and Puzhen Zhang: Software, Investigation, Resources.

Xiaoqian Li and Jiayi Yan: Conceptualization, Methodology, Validation, Writing - review & editing, Supervision.

Zhaobin Sun and Xiaojing Zhu: Conceptualization, Validation, sampling.

Yongjie Wei: Software, Investigation, Resources, Project administration.

Corresponding author

Correspondence to Yongjie Wei.

Ethics declarations

Ethics approval and consent to participate

Not applicable.

Consent for publication

Not applicable.

Competing interests

The authors declare no competing interests.

References

Bi, C., Chen, Y., Zhao, Z., Li, Q., Zhou, Q., Ye, Z., and Ge, X. (2020). Characteristics, sources and health risks of toxic species (PCDD/Fs, PAHs and heavy metals) in $PM_{2.5}$ during fall and winter in an industrial area. Chemosphere 238, 124620.

Bie Shu-jun, Yang Ling-xiao, Gao Ying, Jang Pan, Li Yan-yan, Yang Yu-meng, Zhao Tong, Wag Wen-xing. Characteristics of Atmospheric $PM_{2.5}$ Pollution and Its Influence on Visibility in Background Areas of Ji'nan. Environmental Science, 2019, 40(9): 3868-3874.(in Chinese)

Castro, L.M., Pio, C.A., Harrison, R.M., and Smith, D.J.T. (1999). Carbonaceous aerosol in urban and rural European atmospheres: estimation of secondary organic carbon concentrations. Atmospheric Environment 33, 2771-2781.

Chen, P., Bi, X., Zhang, J., Wu, J., and Feng, Y. (2015). Assessment of heavy metal pollution characteristics and human health risk of exposure to ambient $PM_{2.5}$ in Tianjin, China. Particuology 20, 104-109.

Cheng, M., Tang, G., Lv, B., Li, X., Wu, X., Wang, Y., and Wang, Y. (2021). Source apportionment of $PM_{2.5}$ and visibility in Jinan, China. Journal of Environmental Sciences 102, 207-215.

Chow, J.C., Watson, J.G., Lu, Z., Lowenthal, D.H., Frazier, C.A., Solomon, P.A., Thuillier, R.H., and Magliano, K. (1996). Descriptive analysis of $PM_{2.5}$ and PM_{10} at regionally representative locations during SJVAQS/AUSPEX. Atmospheric Environment 30, 2079-2112.

Ding, A., Huang, X., Nie, W., Chi, X., Fu, C.J.A.C., and Physics (2019). Significant reduction of $PM_{2.5}$ in eastern China due to regional-scale emission control: Evidences from the SORPES station, 2011–2018. 1-21.

Dong, Z., Su, F., Zhang, Z., and Wang, S. (2020). Observation of chemical components of $PM_{2.5}$ and secondary inorganic aerosol formation during haze and sandy haze days in Zhengzhou, China. Journal of Environmental Sciences 88, 316-325.

Du, J., Zhang, X., Huang, T., Gao, H., Mo, J., Mao, X., and Ma, J. (2019). Removal of $PM_{2.5}$ and secondary inorganic aerosols in the North China Plain by dry deposition. Science of The Total Environment 651, 2312-2322.

Feng, J., Yu, H., Su, X., Liu, S., Li, Y., Pan, Y., and Sun, J.-H. (2016). Chemical composition and source apportionment of $PM_{2.5}$ during Chinese Spring Festival at Xinxiang, a heavily polluted city in North China: Fireworks and health risks. Atmospheric Research 182, 176-188.

Gao Yanxin, Sui Shaofeng, Kong Fanling, Wang Yan, Wang Guoling, and Shao Lijun. Characteristic analysis and evaluation of heavy metal pollution in atmospheric $PM_{2.5}$ in main urban area of Jinan City[J]. Journal of Environmental & Occupational Medicine, 2019, 36(11):1042-1048. (in Chinese)

Guo, B., Wang, Y., Zhang, X., Che, H., Zhong, J., Chu, Y., and Cheng, L. (2020a). Temporal and spatial variations of haze and fog and the characteristics of $PM_{2.5}$ during heavy pollution episodes in China from 2013 to 2018. Atmospheric Pollution Research 11, 1847-1856.

Guo, H., Li, W., Yao, F., Wu, J., Zhou, X., Yue, Y., and Yeh, A.G.O. (2020b). Who are more exposed to $PM_{2.5}$ pollution: A mobile phone data approach. Environment International 143, 105821.

Hao, Y., Gao, C., Deng, S., Yuan, M., Song, W., Lu, Z., and Qiu, Z. (2019). Chemical characterisation of $PM_{2.5}$ emitted from motor vehicles powered by diesel, gasoline, natural gas and methanol fuel. Science of The Total Environment 674, 128-139.

He, J., Zhang, L., Yao, Z., Che, H., Gong, S., Wang, M., Zhao, M., and Jing, B. (2020). Source apportionment of particulate matter based on numerical simulation during a severe pollution period in Tangshan, North China. Environmental Pollution 266, 115133.

HJ 799-2016. Ambient Air-Determination of the water soluble anions F^-、Cl^-、Br^-、NO_2^-、NO_3^-、PO_4^{3-}、SO_3^{2-}、SO_4^{2-}、from atmospheric particles-Ion chromatography[S]. 2016

HJ 800-2016. Ambient Air-Determination of the water soluble cations (Li^+, Na^+, NH_4^+, K^+, Ca^{2+}, Mg^{2+}) from atmospheric particles-Ion chromatography [S]. 2016.

Honda, A., Okuda, T., Nagao, M., Miyasaka, N., Tanaka, M., and Takano, H. (2020). $PM_{2.5}$ collected using cyclonic separation causes stronger biological responses than that collected using a conventional filtration method. Environmental Research, 110490.

Hu, W., Zhao, T., Bai, Y., Kong, S., Xiong, J., Sun, X., Yang, Q., Gu, Y., and Lu, H. (2021). Importance of regional $PM_{2.5}$ transport and precipitation washout in heavy air pollution in the Twain-Hu Basin over Central China: Observational analysis and WRF-Chem simulation. Science of The Total Environment 758, 143710.

Ikemori, F., Uranishi, K., Sato, T., Fujihara, M., Hasegawa, H., and Sugata, S. (2021). Time-resolved characterization of organic compounds in $PM_{2.5}$ collected at Oki Island, Japan, affected by transboundary pollution of biomass and non-biomass burning from Northeast China. Science of The Total Environment 750, 142183.

Jain, S., Sharma, S.K., Vijayan, N., and Mandal, T.K. (2020). Seasonal characteristics of aerosols ($PM_{2.5}$ and PM_{10}) and their source apportionment using PMF: A four year study over Delhi, India. Environmental Pollution 262, 114337.

Jia, B., Wang, Y., Wang, C., Zhang, Q., Gao, M., and Yung, K.K.L. (2021). Sensitivity of $PM_{2.5}$ to NOx emissions and meteorology in North China based on observations. Science of The Total Environment 766, 142275.

Jiang, H., Geng, X., Cheng, Z., Zhan, L., Tang, J., Li, J., Xiao, H., Song, H., Wang, T., Li, J., et al. (2021). Source apportionment of $PM_{2.5}$ carbonaceous aerosols during a long-lasting winter haze episode in Xiangyang, central China. Atmospheric Pollution Research 12, 470-479.

Khan, J.Z., Sun, L., Tian, Y., Shi, G., and Feng, Y. (2021). Chemical characterization and source apportionment of PM_1 and $PM_{2.5}$ in Tianjin, China: Impacts of biomass burning and primary biogenic sources. Journal of Environmental Sciences 99, 196-209.

Li, F., Yan, J., Wei, Y., Zeng, J., Wang, X., Chen, X., Zhang, C., Li, W., Chen, M., and Lü, G. (2021). $PM_{2.5}$-bound heavy metals from the major cities in China: Spatiotemporal distribution, fuzzy exposure assessment and health risk management. Journal of Cleaner Production 286, 124967.

Li, M., Wang, L., Liu, J., Gao, W., Song, T., Sun, Y., Li, L., Li, X., Wang, Y., Liu, L., et al. (2020a). Exploring the regional pollution characteristics and meteorological formation mechanism of $PM_{2.5}$ in North China during 2013–2017. Environment International 134, 105283.

Li, Q., Wu, B., Liu, J., Zhang, H., Cai, X., and Song, Y. (2020b). Characteristics of the atmospheric boundary layer and its relation with $PM_{2.5}$ during haze episodes in winter in the North China Plain. Atmospheric Environment 223, 117265.

Lim, S., Yang, X., Lee, M., Li, G., Gao, Y., Shang, X., Zhang, K., Czimczik, C.I., Xu, X., Bae, M.-S., et al. (2020). Fossil-driven secondary inorganic $PM_{2.5}$ enhancement in the North China Plain: Evidence from carbon and nitrogen isotopes. Environmental Pollution 266, 115163.

Lin, C.Q., Liu, G., Lau, A.K.H., Li, Y., Li, C.C., Fung, J.C.H., and Lao, X.Q. (2018). High-resolution satellite remote sensing of provincial $PM_{2.5}$ trends in China from 2001 to 2015. Atmospheric Environment 180, 110-116.

LIU Xiao-di, MENG Jing-jing, HOU Zhan-fang, LI Jing, XING Ji-zhao, WEI Ben-jie, ZHANG Er-xun, LIU Jia-zhen, DONG Jie. Analysis of Seasonal Variations in Chemical Characteristics and Sources of $PM_{2.5}$ During Summer and Winter in Ji'nan City. Environmental Science, 2018, 39(9): 4014-4025. (in Chinese)

Liu, F., Tan, Q., Jiang, X., Yang, F., and Jiang, W. (2019). Effects of relative humidity and $PM_{2.5}$ chemical compositions on visibility impairment in Chengdu, China. Journal of Environmental Sciences 86, 15-23.

Liu, S., Xing, J., Westervelt, D.M., Liu, S., Ding, D., Fiore, A.M., Kinney, P.L., Zhang, Y., He, M.Z., Zhang, H., et al. (2021a). Role of emission controls in reducing the 2050 climate change penalty for $PM_{2.5}$ in China. Science of The Total Environment 765, 144338.

Liu, Y., Li, C., Zhang, C., Liu, X., Qu, Y., An, J., Ma, D., Feng, M., and Tan, Q. (2021b). Chemical characteristics, source apportionment, and regional contribution of $PM_{2.5}$ in Zhangjiakou, Northern China: A multiple sampling sites observation and modeling perspective. Environmental Advances 3, 100034.

Luo, L., Tian, H., Liu, H., Bai, X., Liu, W., Liu, S., Wu, B., Lin, S., Zhao, S., Hao, Y., et al. (2021). Seasonal variations in the mass characteristics and optical properties of carbonaceous constituents of $PM_{2.5}$ in six cities of North China. Environmental Pollution 268, 115780.

Lurie, K., Nayebare, S.R., Fatmi, Z., Carpenter, D.O., Siddique, A., Malashock, D., Khan, K., Zeb, J., Hussain, M.M., Khatib, F., et al. (2019). $PM_{2.5}$ in a megacity of Asia (Karachi): Source apportionment and health effects. Atmospheric Environment 202, 223-233.

Lv, L., Chen, Y., Han, Y., Cui, M., Wei, P., Zheng, M., and Hu, J. (2021). High-time-resolution $PM_{2.5}$ source apportionment based on multi-model with organic tracers in Beijing during haze episodes. Science of The Total Environment 772, 144766.

Lv, L., Liu, W., Zhang, T., Chen, Z., Dong, Y., Fan, G., Xiang, Y., Yao, Y., Yang, N., Chu, B., et al. (2017). Observations of particle extinction, $PM_{2.5}$ mass concentration profile and flux in north China based on mobile lidar technique. Atmospheric Environment 164, 360-369.

Manousakas, M., Papaefthymiou, H., Diapouli, E., Migliori, A., Karydas, A.G., Bogdanovic-Radovic, I., and Eleftheriadis, K. (2017). Assessment of $PM_{2.5}$ sources and their corresponding level of uncertainty in a coastal urban area using EPA PMF 5.0 enhanced diagnostics. Science of The Total Environment 574, 155-164.

Ministry of Ecological Environment. Exposure Factors Handbook of Chinese Population. Beijing: China Environmental Science Press, 2013:156-164.

Nguyen, G.T.H., Shimadera, H., Uranishi, K., Matsuo, T., and Kondo, A. (2019). Numerical assessment of $PM_{2.5}$ and O3 air quality in Continental Southeast Asia: Impacts of potential future climate change. Atmospheric Environment 215, 116901.

Padoan, S., Zappi, A., Adam, T., Melucci, D., Gambaro, A., Formenton, G., Popovicheva, O., Nguyen, D.-L., Schnelle-Kreis, J., and Zimmermann, R. (2020). Organic molecular markers and source contributions in a polluted municipality of north-east Italy: Extended PCA-PMF statistical approach. Environmental Research 186, 109587.

Pandolfi, M., Amato, F., Reche, C., Alastuey, A., Otjes, R.P., Blom, M.J., Querol, X.J.A.C., and Physics (2012). Summer ammonia measurements in a densely populated Mediterranean city. 12, 7557-7575.

Ren, Y., Wei, J., Wu, Z., Ji, Y., Bi, F., Gao, R., Wang, X., Wang, G., and Li, H. (2021). Chemical components and source identification of $PM_{2.5}$ in non-heating season in Beijing: The influences of biomass burning and dust. Atmospheric Research 251, 105412.

Sawlani, R., Agnihotri, R., and Sharma, C. (2021). Chemical and isotopic characteristics of $PM_{2.5}$ over New Delhi from September 2014 to May 2015: Evidences for synergy between air-pollution and meteorological changes. Science of The Total Environment 763, 142966.

Shi, C., Nduka, I.C., Yang, Y., Huang, Y., Yao, R., Zhang, H., He, B., Xie, C., Wang, Z., and Yim, S.H.L. (2020). Characteristics and meteorological mechanisms of transboundary air pollution in a persistent heavy $PM_{2.5}$ pollution episode in Central-East China. Atmospheric Environment 223, 117239.

Srinivas, B., and Sarin, M.M. (2014). $PM_{2.5}$, EC and OC in atmospheric outflow from the Indo-Gangetic Plain: Temporal variability and aerosol organic carbon-to-organic mass conversion factor. Science of The Total Environment 487, 196-205.

Sugiyama, T., Ueda, K., Seposo, X.T., Nakashima, A., Kinoshita, M., Matsumoto, H., Ikemori, F., Honda, A., Takano, H., Michikawa, T., et al. (2020). Health effects of $PM_{2.5}$ sources on children's allergic and respiratory symptoms in Fukuoka, Japan. Science of The Total Environment 709, 136023.

Turpin, B.J., and Huntzicker, J.J. (1995). Identification of secondary organic aerosol episodes and quantitation of primary and secondary organic aerosol concentrations during SCAQS. Atmospheric Environment 29, 3527-3544.

USEPA, 1989. Risk assessment guidance for superfund volume □: Human health evaluation manual (part A) [R]. Washington. DC: USEPA, Office of Emergency and Remedical Response.

Van Donkelaar, A., Martin, R.V., Brauer, M., Kahn, R., Levy, R., Verduzco, C., and Villeneuve, P.J.J.E.H.P. (2010). Global Estimates of Ambient Fine Particulate Matter Concentrations from Satellite-Based Aerosol Optical Depth: Development and Application. 118, 847-855.

Wang, H., Wang, X., Zhou, H., Ma, H., Xie, F., Zhou, X., Fan, Q., Lü, C., and He, J. (2021). Stoichiometric characteristics and economic implications of water-soluble ions in $PM_{2.5}$ from a resource-dependent city. Environmental Research 193, 110522.

Wang, S., Wang, L., Wang, N., Ma, S., Su, F., and Zhang, R. (2020). Formation of droplet-mode secondary inorganic aerosol dominated the increased $PM_{2.5}$ during both local and transport haze episodes in Zhengzhou, China. Chemosphere, 128744.

Wang, S., Yu, R., Shen, H., Wang, S., Hu, Q., Cui, J., Yan, Y., Huang, H., and Hu, G. (2019a). Chemical characteristics, sources, and formation mechanisms of $PM_{2.5}$ before and during the Spring Festival in a coastal city in Southeast China. Environmental Pollution 251, 442-452.

Wang, Y., Duan, X., Wang, L.J.I.J.o.E.R., and Health, P. (2019b). Spatial-Temporal Evolution of $PM_{2.5}$ Concentration and its Socioeconomic Influence Factors in Chinese Cities in 2014–2017. 16.

Wang, Zhanshan, Li, Lingjun, Pan, Libo, Jinxiang, Sun, Feng, and Society, L.J.B.o.t.A.M. (2016). SCIENCE-POLICY INTERPLAY Improvement of Air Quality from 2008 to 2014 in Beijing and the Scientific Approach to Achieve APEC Blue. Bulletin of the American Meteorological Society 2, 553-559.

Wei, Y., Chen, H., Sun, H., Zhang, F., Shang, X., Yao, L., Zheng, H., Li, Q., and Chen, J. (2020). Nocturnal $PM_{2.5}$ explosive growth dominates severe haze in the rural North China Plain. Atmospheric Research 242, 105020.

Wu, X., Xin, J., Zhang, X., Klaus, S., Wang, Y., Wang, L., Wen, T., Liu, Z., Si, R., Liu, G., et al. (2020). A new approach of the normalization relationship between $PM_{2.5}$ and visibility and the theoretical threshold, a case in north China. Atmospheric Research 245, 105054.

Yang, L., Wang, S., Duan, S., Yan, Q., Jiang, N., Zhang, R., and Li, S. (2020). Characteristics and formation mechanisms of secondary inorganic ions in $PM_{2.5}$ during winter in a central city of China: Based on a high time resolution data. Atmospheric Research 233, 104696.

Yang, Q., Wang, H., Wang, J., Lu, M., Liu, C., Xia, X., Yin, W., and Guo, H. (2018). $PM_{2.5}$-bound SO_4^{2-} absorption and assimilation of poplar and its physiological responses to $PM_{2.5}$ pollution. Environmental and Experimental Botany 153, 311-319.

Yao, L., Yang, L., Yuan, Q., Yan, C., Dong, C., Meng, C., Sui, X., Yang, F., Lu, Y., and Wang, W. (2016). Sources apportionment of $PM_{2.5}$ in a background site in the North China Plain. Science of The Total Environment 541, 590-598.

Yi, Y., Meng, J., Hou, Z., Wang, G., Zhou, R., Li, Z., Li, Y., Chen, M., Liu, X., Li, H., et al. (2021). Contrasting compositions and sources of organic aerosol markers in summertime $PM_{2.5}$ from urban and mountainous regions in the North China Plain. Science of The Total Environment 766, 144187.

Yin, X., Fan, G., Liu, J., Jiang, T., and Wang, L.J.E.F. (2020). Characteristics of heavy metals and persistent organic pollutants in $PM_{2.5}$ in two typical industrial cities, North China. 1-9.

Zhai, Y., Liu, X., Chen, H., Xu, B., Zhu, L., Li, C., and Zeng, G. (2014). Source identification and potential ecological risk assessment of heavy metals in $PM_{2.5}$ from Changsha. Science of The Total Environment 493, 109-115.

Zhang Linlin, Xue Lidong, Lu Yibing, Xu Renji, Teng Enjiang, Li Guogang.APEC Health Risk Assessment of Heavy Metals in Fine Particulate Matter in Urban Air [J]. Environmental Chemistry, 2015, 34(06):1218-1220. (in Chinese)

Zhang Wenjuan, Li Min, Fu Huaxuan, etc. Analysis of Chemical Constituents and Pollution Characteristics of $PM_{2.5}$ in Jinan [J]. Environmental Pollution & Control, 2019, 41(12):1490. (in Chinese)

Zhang, X., Gu, X., Cheng, C., and Yang, D. (2020a). Spatiotemporal heterogeneity of $PM_{2.5}$ and its relationship with urbanization in North China from 2000 to 2017. Science of The Total Environment 744, 140925.

Zhang, B., Wu, B., and Liu, J. (2020b). $PM_{2.5}$ pollution-related health effects and willingness to pay for improved air quality: Evidence from China's prefecture-level cities. Journal of Cleaner Production 273, 122876.

Zhang, X., Lyu, J., Han, Y., Sun, N., Sun, W., Li, J., Liu, C., and Yin, S. (2020c). Effects of the leaf functional traits of coniferous and broadleaved trees in subtropical monsoon regions on $PM_{2.5}$ dry deposition velocities. Environmental Pollution 265, 114845.

Zhang, Y.-x., Shao, M., Zhang, Y.-h., Zeng, L.-m., He, L.-y., Zhu, B., Wei, Y.-j., and Zhu, X.-l. (2007). Source profiles of particulate organic matters emitted from cereal straw burnings. Journal of Environmental Sciences 19, 167-175.

Zhao, C., Wang, Y., Su, Z., Pu, W., Niu, M., Song, S., Wei, L., Ding, Y., Xu, L., Tian, M., et al. (2020a). Respiratory exposure to $PM_{2.5}$ soluble extract disrupts mucosal barrier function and promotes the development of experimental asthma. Science of The Total Environment 730, 139145.

Zhao, X., Zhao, X., Liu, P., Ye, C., Xue, C., Zhang, C., Zhang, Y., Liu, C., Liu, J., Chen, H., et al. (2020b). Pollution levels, composition characteristics and sources of atmospheric $PM_{2.5}$ in a rural area of the North China Plain during winter. Journal of Environmental Sciences 95, 172-182.

Zong, Z., Wang, X., Tian, C., Chen, Y., Fu, S., Qu, L., Ji, L., Li, J., and Zhang, G. (2018). PMF and PSCF based source apportionment of $PM_{2.5}$ at a regional background site in North China. Atmospheric Research 203, 207-215.

The English in this document has been checked by at least two professional editors, both native speakers of English. For a certificate, please see:

http://www.textcheck.com/certificate/fuijGg

Figures

Figure 1

Location of the monitoring site. (A) The global PM2.5 distribution from 2001 to 2006 based on satellite observations by the United States National Aeronautics and Space Administration (Van Donkelaar et al., 2010). (B) The national PM2.5 distribution in China based on monitoring data from 1436 sites from 2014

to 2017 (Wang et al., 2019b). (C) Administrative map of Jinan City, with different colors indicating counties. The black triangle represents the location of the monitoring site used in this study.

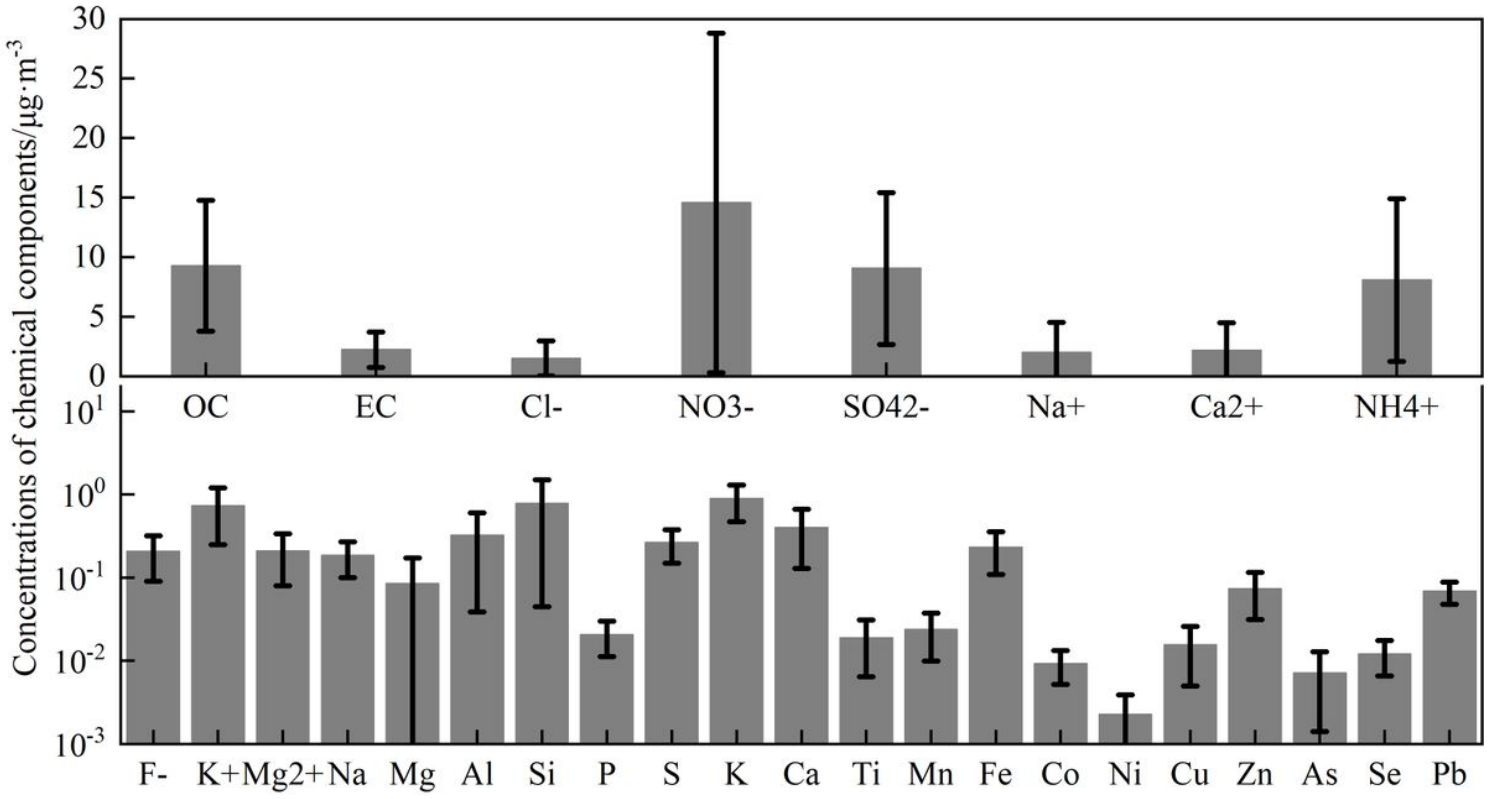

Figure 2

Average concentrations of the chemical components of PM2.5 during the sampling period

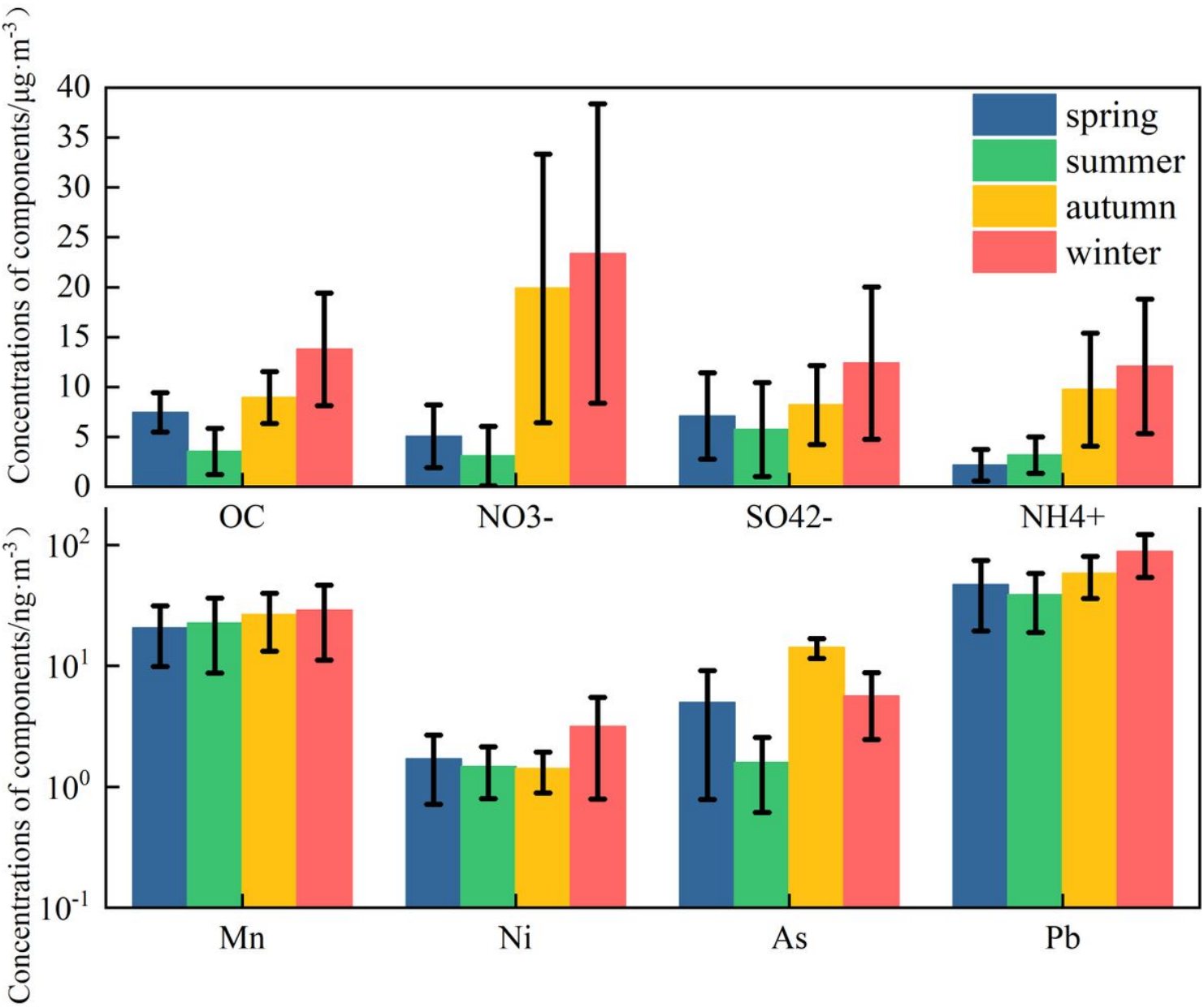

Figure 3

Concentrations of the chemical components of PM2.5 in different seasons

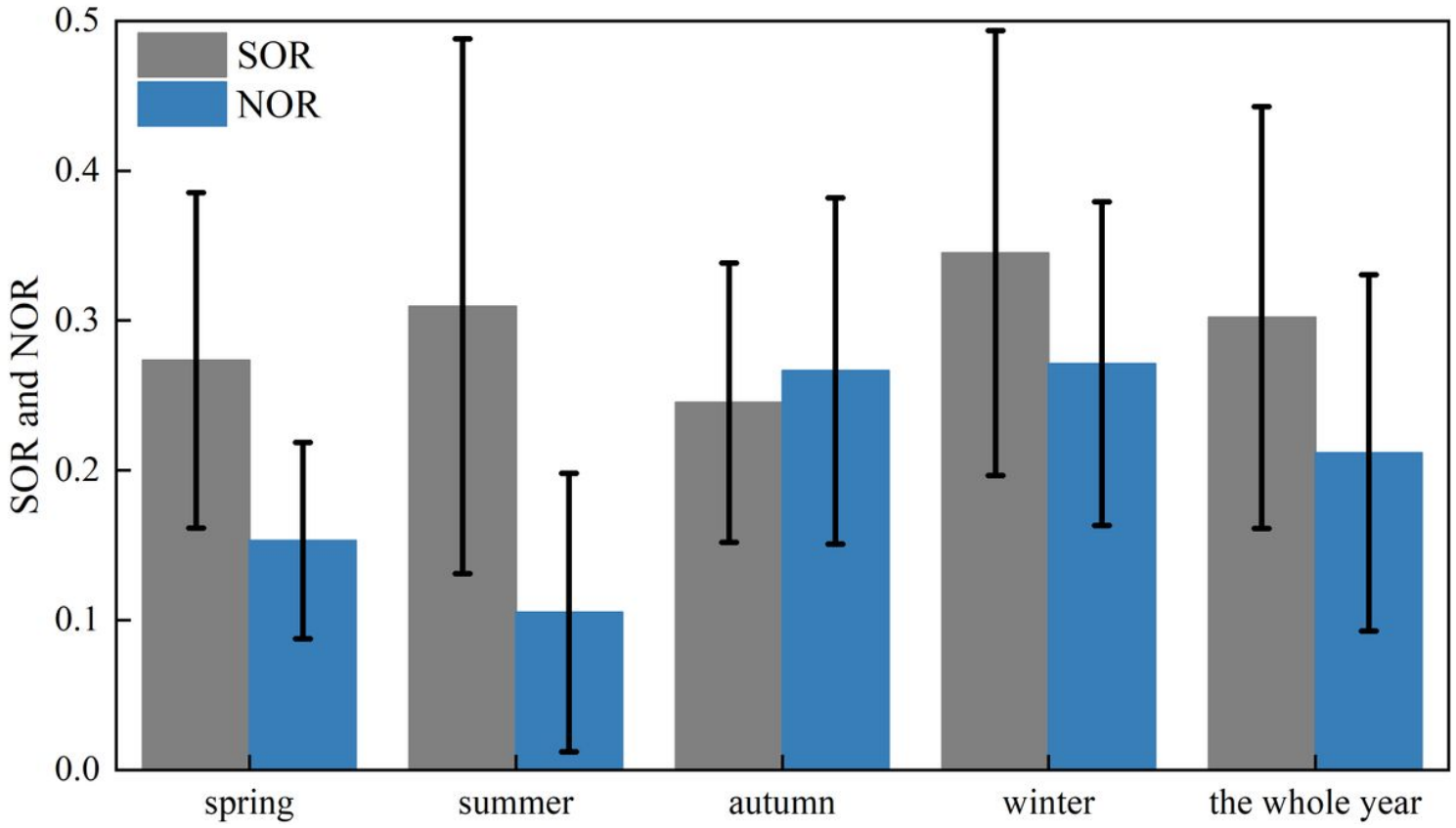

Figure 4

The SOR and NOR in different seasons

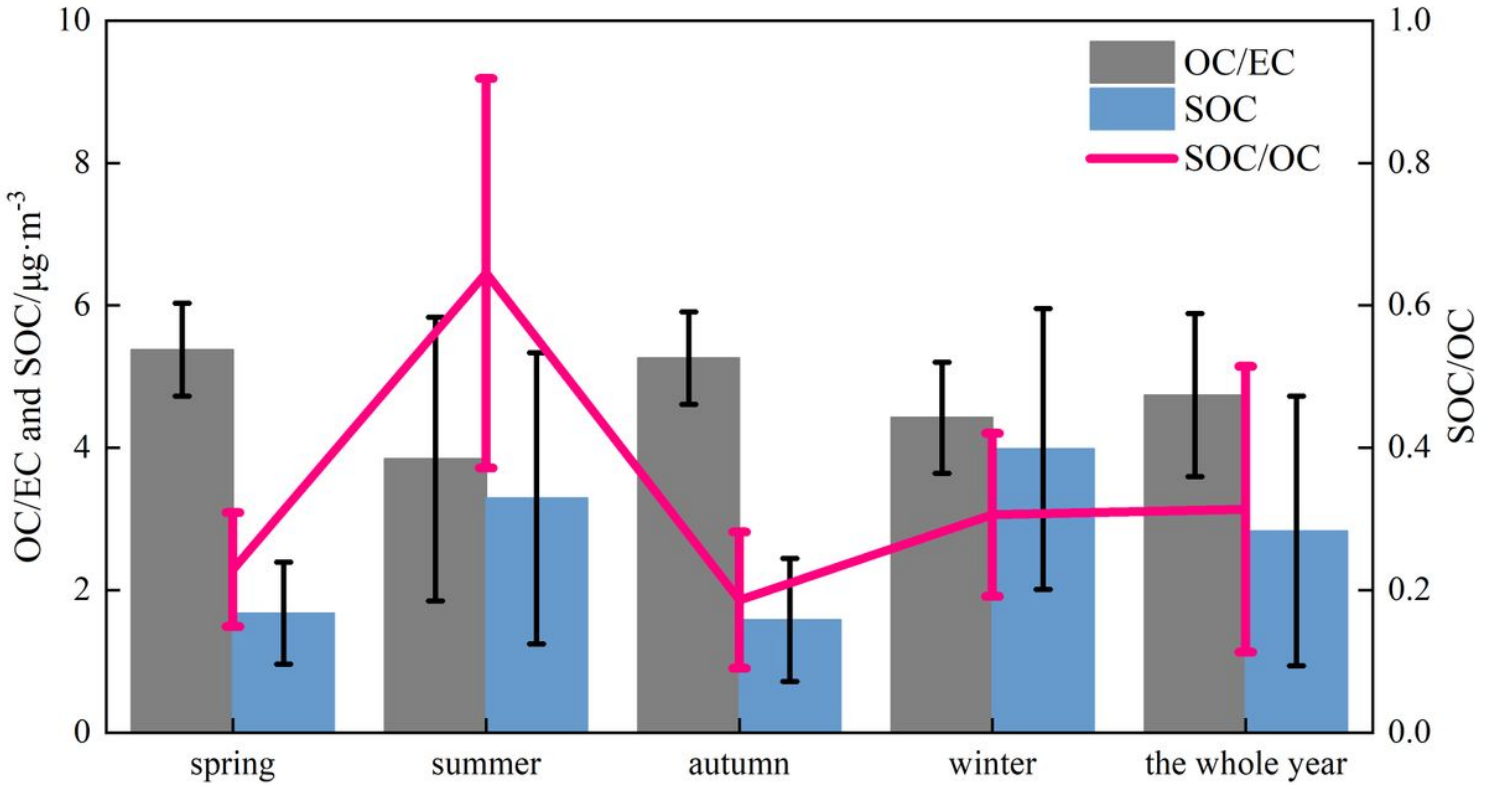

Figure 5

The OC/EC ratio, SOC concentration, and SOC/OC ratio in different seasons

Figure 6

Non-carcinogenic and carcinogenic risk coefficients for As, Mn, Ni, and Pb

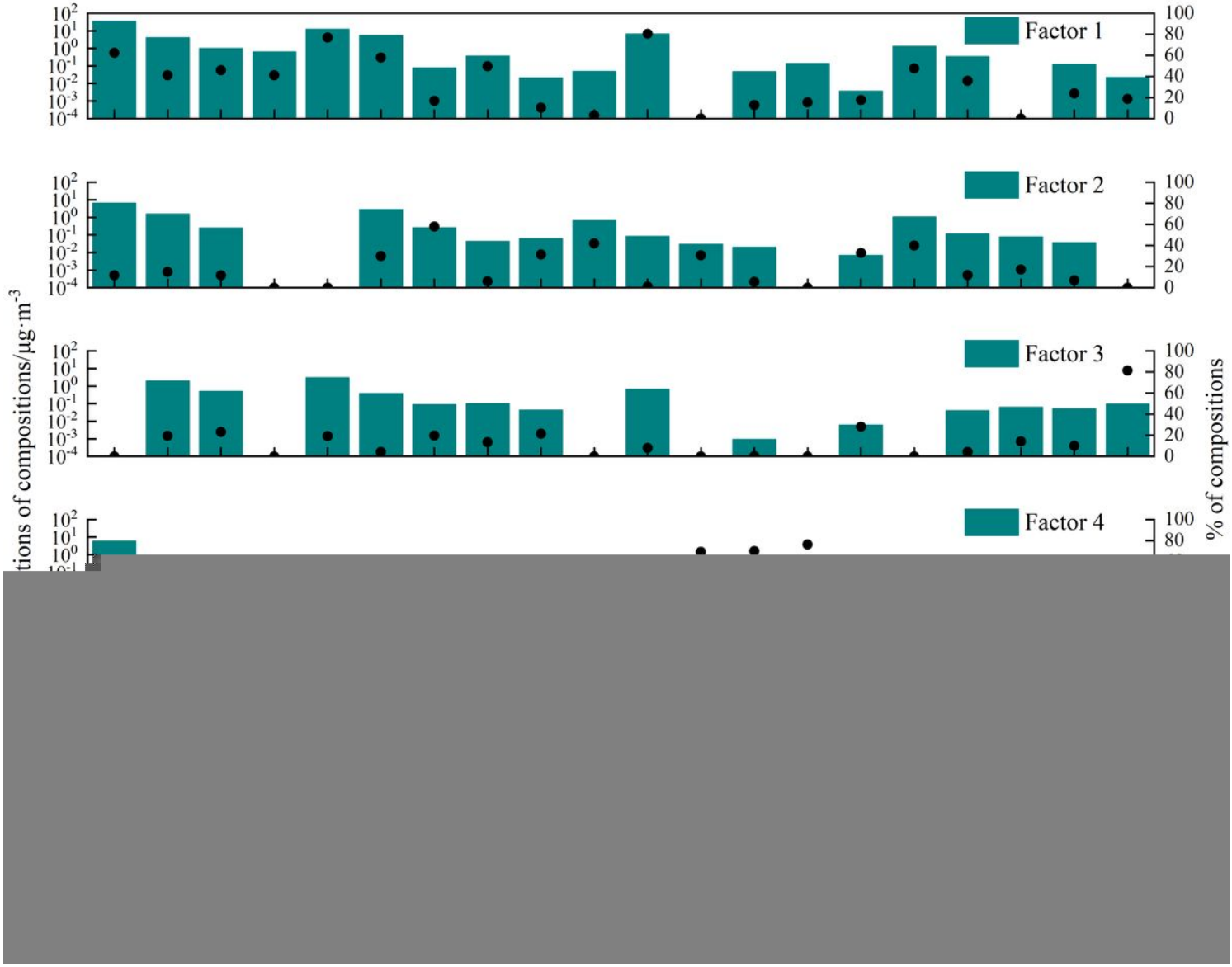

Figure 7

Five source profiles (bars) and contribution percentages (dots) from each source factor resolved from the PMF model.

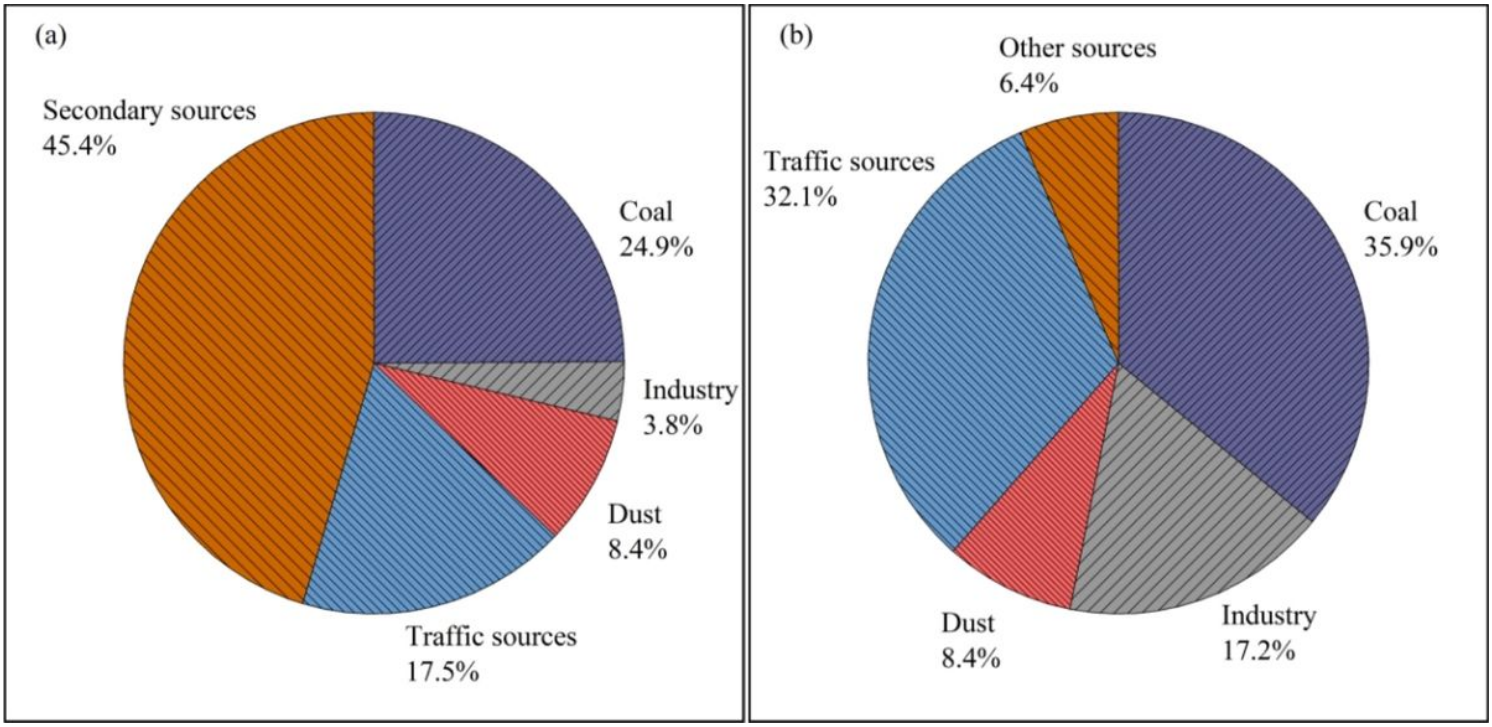

Figure 8

Source analysis of PM2.5 in Pingyin County. (a) PMF results for source contributions. (b) Source analysis results after secondary apportionment